Maria Lucia Sambataro

Relativistic transport approach for charm and bottom toward a phenomenological determination of Ds

In collaboration with: V. Minissale, Y. Sun, S. Plumari, G. Parisi, V. Greco

Dipartimento di Fisica e Astronomia 'E.Majorana'- Università degli Studi di Catania

INFN -Laboratori Nazionali del Sud (LNS)

Meeting SIM - Catania INFN (LNS) - 10-11 Settembre 2024

Basic scales of charm and bottom quarks

Charm M_c≈1.3 GeV and Bottom M_b≈4.2 GeV

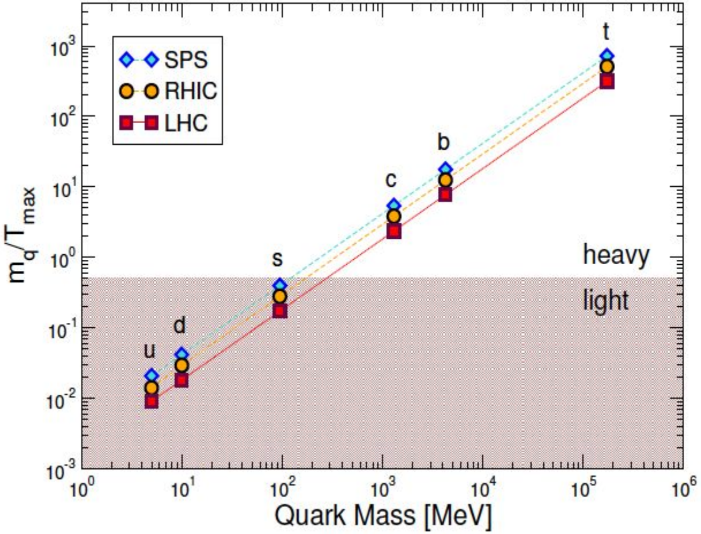

- $m_{c,b} >> \Lambda_{QCD}$
  pQCD initial production
- $m_{c,b} >> T_{RHIC,LHC}$
  negligible thermal production
- $\tau_0 < 0{,}08$ fm/c << τ_{QGP}
- $\tau_{th} \approx \tau_{QGP} >> \tau_{g,q}$

They experience the full evolution of the QGP.

They carry more informations with respect to their light counterparts.

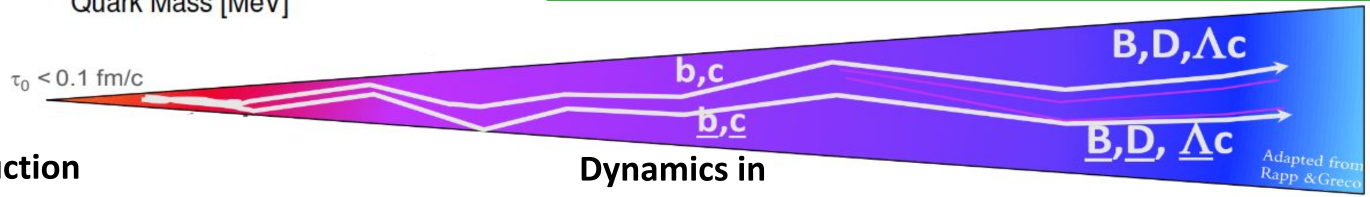

Initial production

Dynamics in QGP

Hadronization:
Final hadron Spectra and observables

Reviews:
1. X.Dong, V. Greco Prog. Part. Nucl. Phys. 104 (2019),
2. A.Andronic EPJ C76 (2016), 3) R.Rapp, F.Prino J.Phys. G43 (2016)

CATANIA MODEL: QUASI-PARTICLE MODEL AND TRANSPORT THEORY

Quasi Particle Model (QPM) fitting lQCD

Non perturbative dynamics → M scattering matrices (q,g → Q) evaluated by Quasi-Particle Model fit to **lQCD thermodynamics**

N_f=2+1
Bulk:
u,d,s

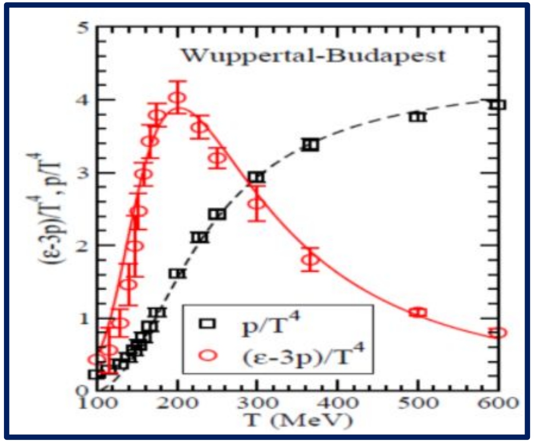

$$m_g^2(T) = \frac{2N_c}{N_c^2-1} g^2(T) T^2$$

$$m_q^2(T) = \frac{1}{N_c} g^2(T) T^2$$

→ **Thermal masses of gluons and light quarks**

g(T) from a fit to ε from lQCD data → good reproduction of P, ε-3P

$$g^2(T) = \frac{48\pi^2}{(11N_c - 2N_f)\ln\left[\lambda\left(\frac{T}{T_c} - \frac{T_s}{T_c}\right)\right]^2}$$

λ=2.6
T_s=0.57 T_c

Larger than pQCD especially as T → T_c

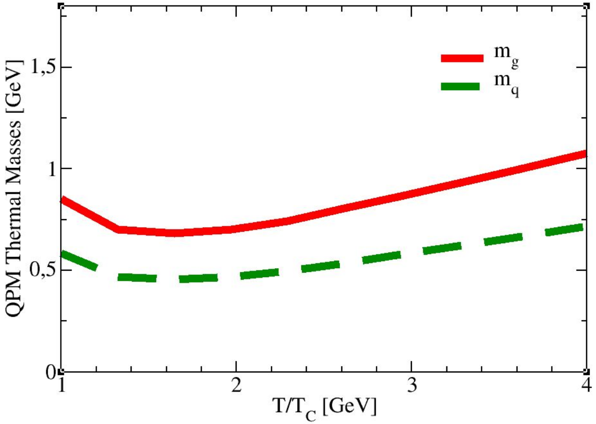

S. Plumari et al, *Phys.Rev.D* 84 (2011) 094004
H. Berrehrah,, PHYSICAL REVIEW C **93**, 044914 (2016)

Relativistic Boltzmann equation at finite η/s

Bulk evolution

$$p^{\mu}\partial_{\mu}f_q(x,p)+m(x)\partial^{x}_{\mu}m(x)\partial^{\mu}_{p}f_q(x,p)=C[f_q,f_g]$$
$$p^{\mu}\partial_{\mu}f_g(x,p)+m(x)\partial^{x}_{\mu}m(x)\partial^{\mu}_{p}f_g(x,p)=C[f_q,f_g]$$

Free-streaming | field interaction $\varepsilon - 3p \neq 0$ | Collision term gauged to some η/s≠ 0

Equivalent to viscous hydro at η/s ≈ 0.1

HQ evolution

$$p^{\mu}\partial_{\mu}f_Q(x,p)=C[f_q,f_g,f_Q]$$

$$C[f_q,f_g,f_Q]=\frac{1}{2E_1}\int\frac{d^3p_2}{2E_2(2\pi)^3}\int\frac{d^3p_1'}{2E_1'(2\pi)^3}$$
$$\times[f_Q(p_1')f_{q,g}(p_2')-f_Q(p_1)f_{q,g}(p_2)]$$
$$\times|M_{(q,g)\rightarrow Q}(p_1p_2\rightarrow p_1'p_2')|$$
$$\times(2\pi)^4\delta^4(p_1+p_2-p_1'-p_2')$$

Feynman diagrams at first order pQCD for HQs-bulk interaction:

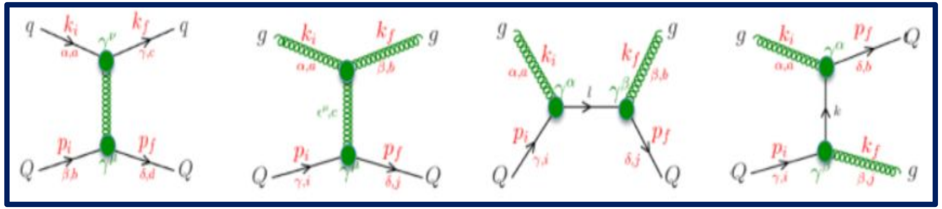

Scattering matrices $M_{g,q}$ by QPM fit to lQCD thermodynamics

HADRONIZATION: hybrid Coalescence + fragmentation

Relativistic Boltzmann equation at finite η/s

Bulk evolution

$$p^{\mu}\partial_{\mu}f_q(x,p)+m(x)\partial^{x}_{\mu}m(x)\partial^{\mu}_{p}f_q(x,p)=C[f_q,f_g]$$
$$p^{\mu}\partial_{\mu}f_g(x,p)+m(x)\partial^{x}_{\mu}m(x)\partial^{\mu}_{p}f_g(x,p)=C[f_q,f_g]$$

Free-streaming — field interaction $\varepsilon - 3p \neq 0$ — Collision term gauged to some η/s≠ 0

Collision Integral gauged to reproduce viscous Hydro at fixed η/s by means of Chapman-Ensksog

$$\sigma(n(\vec{x}),T) = \frac{1}{15}\frac{\langle p\rangle_0}{g(a)n(\vec{x})}\frac{1}{\eta/s}$$

Equivalent to viscous hydro at η/s ≈ 0.1

HQ evolution

$$p^{\mu}\partial_{\mu}f_Q(x,p)=C[f_q,f_g,f_Q]$$

$$C[f_q,f_g,f_Q]=\frac{1}{2E_1}\int\frac{d^3p_2}{2E_2(2\pi)^3}\int\frac{d^3p_1'}{2E_1'(2\pi)^3}$$
$$\times[f_Q(p_1')f_{q,g}(p_2')-f_Q(p_1)f_{q,g}(p_2)]$$
$$\times|M_{(q,g)\to Q}(p_1p_2\to p_1'p_2')|$$
$$\times(2\pi)^4\delta^4(p_1+p_2-p_1'-p_2')$$

Feynman diagrams at first order pQCD for HQs-bulk interaction:

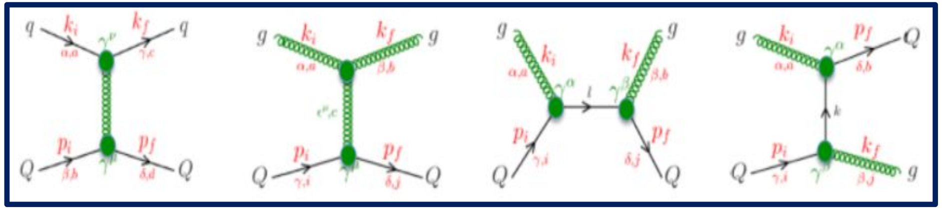

Scattering matrices $M_{g,q}$ by QPM fit to lQCD thermodynamics

HADRONIZATION: hybrid Coalescence + fragmentation

Information from non-equilibrium: anisotropic flows $v_n(p_T)$

$$E\frac{d^3N}{dp_T} = \frac{1}{2\pi}\frac{d^2N}{p_T dp_T dy}\left\{1 + \sum_{i=1}^{\infty} v_n \cos[n(\varphi - \Psi_n)]\right\}$$

Elliptic flow v_2

- **asymmetry** between the **in-plane** and **out-of-plane** directions

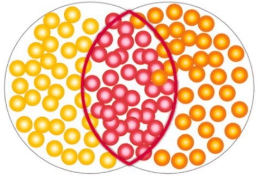

Elliptic flow

Triangular flow v_3

- event-by-event **fluctuations** in the **initial distributions** of nucleons

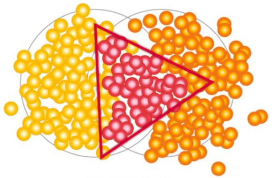

Triangular flow

$$\epsilon_n = \frac{\langle r_\perp^n \cos[n(\varphi - \Phi_n)]\rangle}{\langle r_\perp^n \rangle} \qquad \Phi_n = \frac{1}{n}\arctan\frac{\langle r_\perp^n \sin(n\varphi)\rangle}{\langle r_\perp^n \cos(n\varphi)\rangle}$$

$$r_\perp = \sqrt{x^2 + y^2}, \qquad \varphi = \arctan(y/x)$$

M.L. Sambataro et al., *Eur.Phys.J.C* 82 (2022) 9, 833

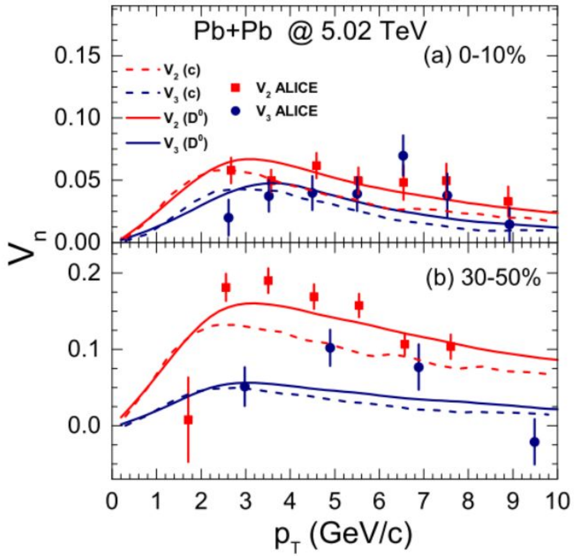

Azimuthal anisotropies depend on

- the interaction and coupling of heavy quarks with the medium;
- the initial conditions of the system, i.e.geometry of the collision;
- **the fluctuations in the distributions of nucleons and gluons within the nuclei**

Monte Carlo Glauber for initial condition of partons

S.Plumari et al, *Phys.Rev.C* 92 (2015) 5

Not almond shape

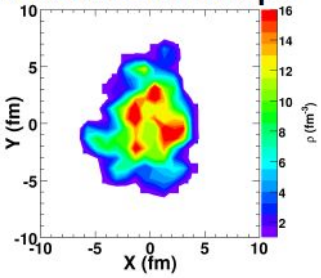

Event-Shape-Engeenering technique

Pb-Pb 5,02 TeV

Selection of events with the same centrality but different initial geometry on the basis of the magnitude of the second-order harmonic reduced flow vector q_2.

$$q_2 = |\vec{Q}_2| / \sqrt{M}$$

$$\vec{Q}_2 = \sum_{j=1}^{M} e^{i2\varphi_j}$$

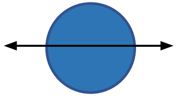

20 % small q_2

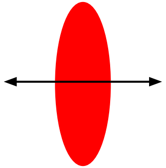

20 % large q_2

Large $q_2 \rightarrow$ large ε_2

$$\epsilon_n = \frac{\langle r_\perp^n \cos[n(\varphi - \Phi_n)] \rangle}{\langle r_\perp^n \rangle} \qquad \Phi_n = \frac{1}{n} \arctan \frac{\langle r_\perp^n \sin(n\varphi) \rangle}{\langle r_\perp^n \cos(n\varphi) \rangle}$$

$$r_\perp = \sqrt{x^2 + y^2}, \qquad \varphi = \arctan(y/x)$$

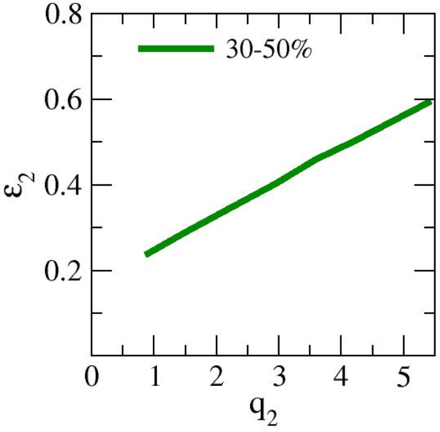

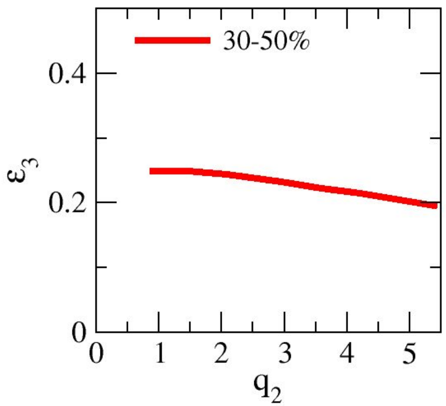

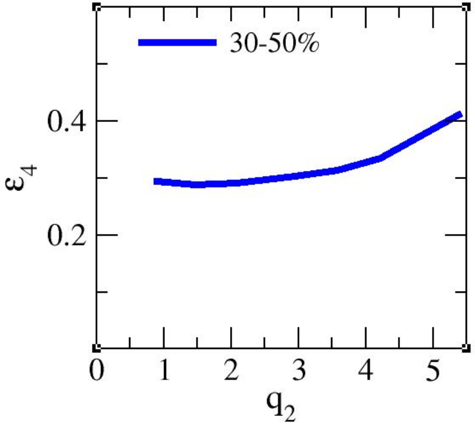

Anti-correlation between ε_2 and ε_3

Non-linear correlation between ε_2 and ε_4

M.L. Sambataro et al., *Eur.Phys.J.C* 82 (2022) 9, 833

ESE: $v_n - v_m$ correlations

M.L. Sambataro, et al., *Eur.Phys.J.C* 82 (2022)

Charged particles

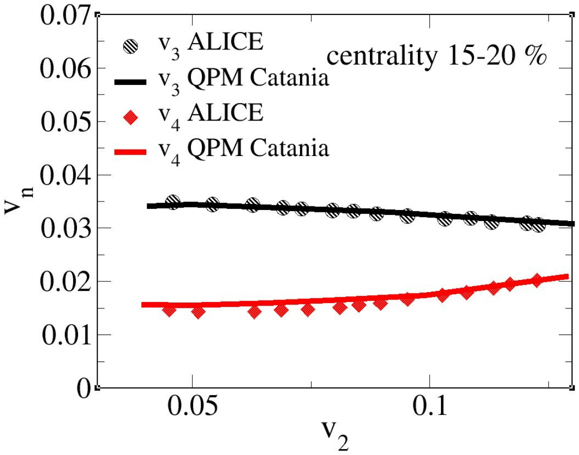

Predictions for D

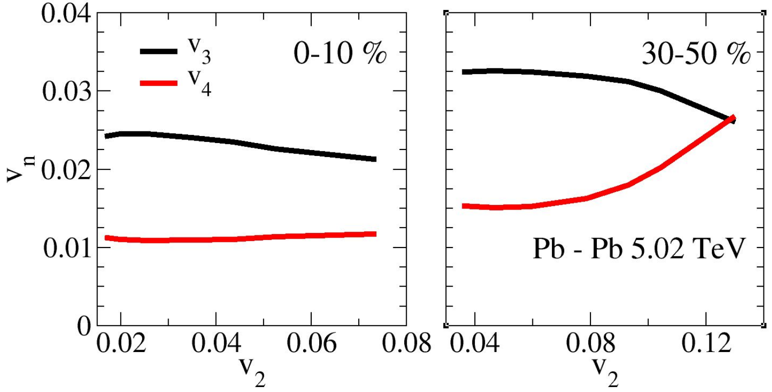

Correlations between the ε_n and ε_m present in the initial geometry → correlations between flow harmonics different orders, i.e. correlations v_n and v_m

- **Good description of v_{n-m} correlation for bulk**
- **Prediction for similar correlation for hard particles**
- **Correlation for D mesons provide insights on the interaction and its temperature dependence**

Plumari et al, Phys.Lett.B 805 (2020) 135460

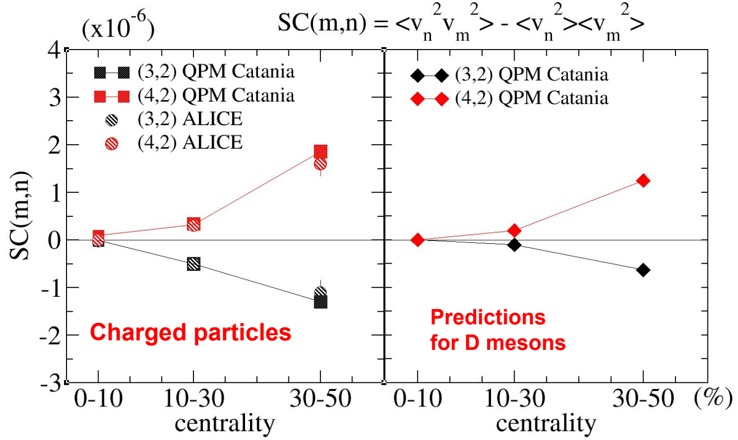

Data taken from: S. Mohapatra *Nucl.Phys.A* 956 (2016) 59-66

Event-shape-engeenering

Selection of events with the same centrality but different initial geometry on the basis of the magnitude of the second-order harmonic reduced flow vector q_2.

$$q_2 = |\vec{Q}_2|/\sqrt{M}$$

$$\vec{Q}_2 = \sum_{j=1}^{M} e^{i2\varphi_j}$$

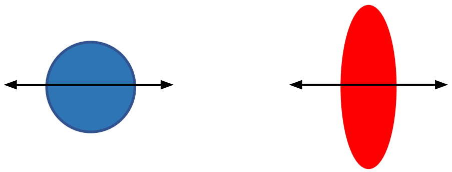

20 % small q_2 20 % large q_2

Large $q_2 \rightarrow$ large ε_2

$$\epsilon_n = \frac{\langle r_\perp^n \cos[n(\varphi - \Phi_n)]\rangle}{\langle r_\perp^n \rangle} \qquad \Phi_n = \frac{1}{n}\arctan\frac{\langle r_\perp^n \sin(n\varphi)\rangle}{\langle r_\perp^n \cos(n\varphi)\rangle}$$

$$r_\perp = \sqrt{x^2 + y^2}, \qquad \varphi = \arctan(y/x)$$

M.L. Sambataro et al., *Eur.Phys.J.C* 82 (2022) 9, 833

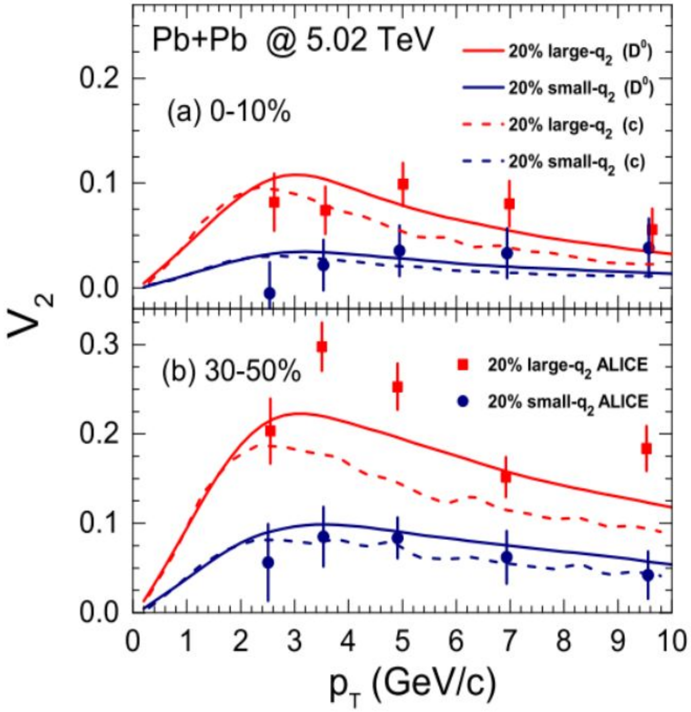

Discrepancy between selected v_2 and unbiased one ~ 50%

Catania QPM: some prediction for charm…

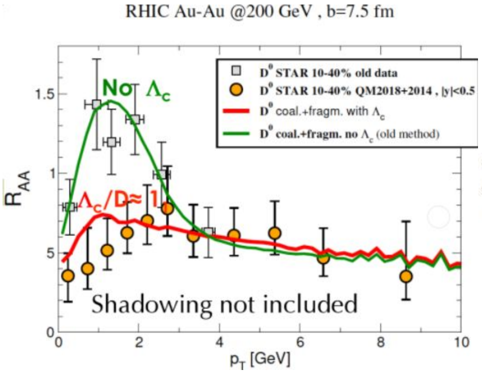

Scardina et al., PRC 97(2017)

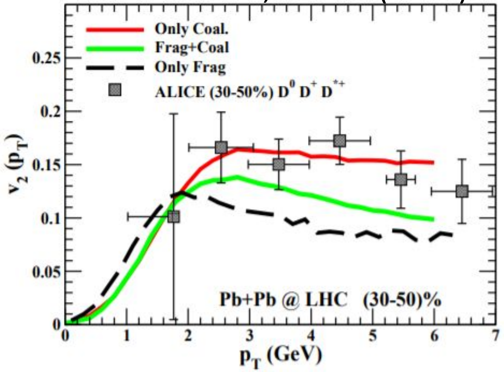

Good description of

R_{AA}, v_2 at RHIC & LHC energies within error bars

Monte Carlo Glauber for initial condition of partons

S.Plumari et al, *Phys.Rev.C* 92 (2015) 5

Predictions for D mesons

- **Event-Shape Engeenering Technique:**
  Prediction for similar correlation for hard particles wrt bulk

v_n - v_m correlations

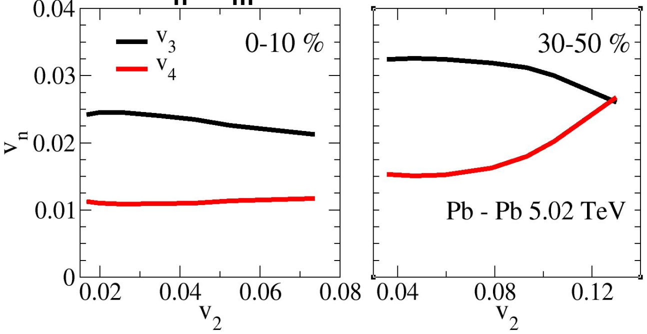

Triangular flow v_3

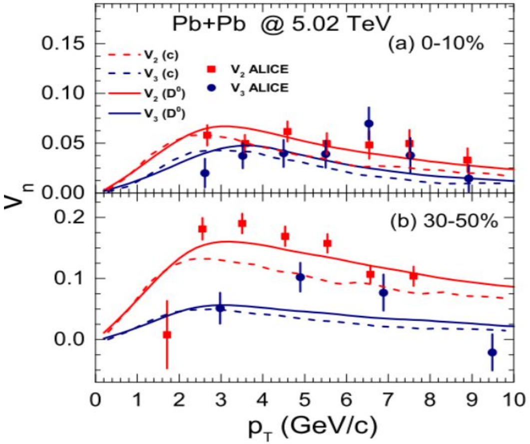

ALICE collaboration, *Phys.Lett.B* 813 (2021) 136054

M.L. Sambataro, et al., *Eur.Phys.J.C* 82 (2022)

Catania QPM: some prediction for charm…

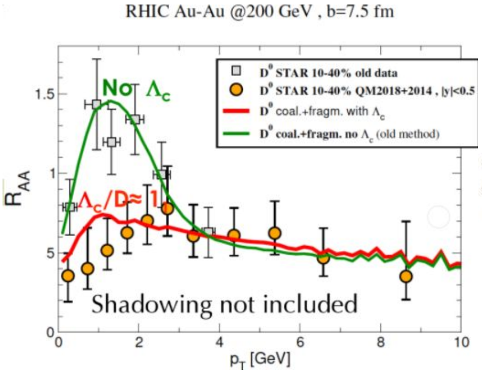

Scardina et al., PRC 97(2017)

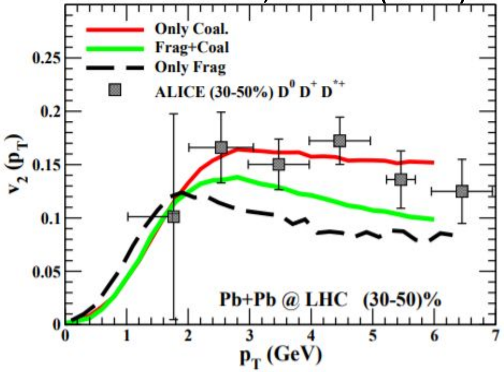

Good description of
R_{AA}, v_2 at RHIC & LHC energies
within error bars

Monte Carlo Glauber for initial condition of partons
S.Plumari et al, *Phys.Rev.C* 92 (2015) 5

- **Event-Shape Engeenering Technique:**
  Prediction for similar correlation for hard particles wrt bulk

Predictions for D mesons

v_n -v_m correlations

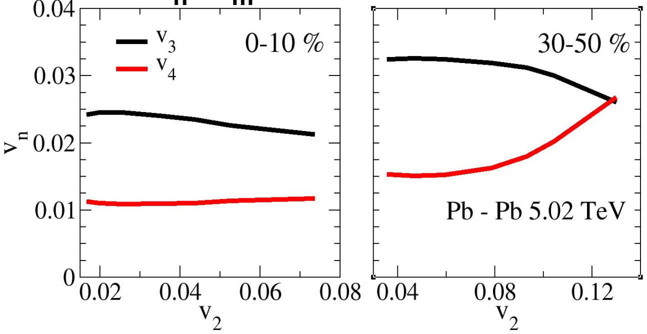

Triangular flow v_3

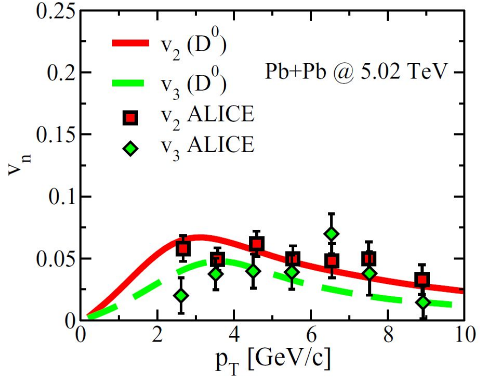

ALICE collaboration, *Phys.Lett.B* 813 (2021) 136054
M.L. Sambataro, et al., *Eur.Phys.J.C* 82 (2022)

[See S. Bass Overview on transport model (03 June 15.15)]

Extension to bottom dynamics: R_{AA}

Hadronization with coalescence + fragmentation model

- ➢ Prediction for B meson R_{AA}
- ➢ R_{AA} of electrons from semileptonic B meson decay

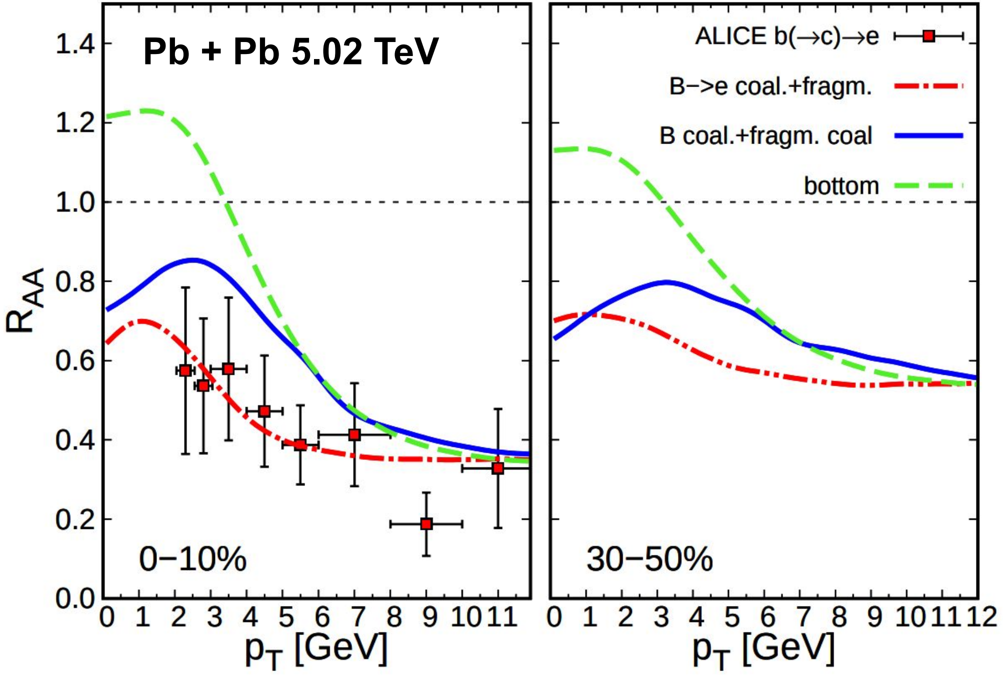

No parameters changed with respect to charm dynamics → same interaction

- Shift of the peak to higher momenta → smaller with respect to the one for D mesons in the same model.

Data from: ALICE coll., arxiv:2211.13985

M.L. Sambataro et al., *Phys.Lett.B* 849 (2024) 138480

Extension to bottom dynamics: $v_{(n=2,3)}$

- Prediction for B meson
- electrons from semileptonic B meson decay within a coal + fragm model

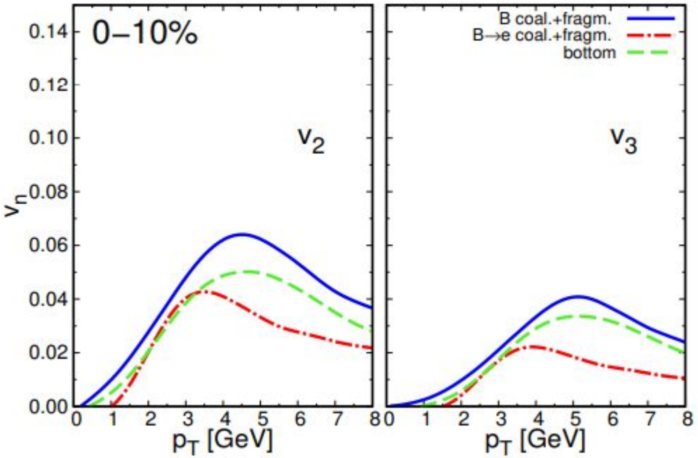

No parameters changed with respect to charm dynamics

M.L. Sambataro et al., *Phys.Lett.B* 849 (2024) 138480

Data from ALICE, PRL 126, 162001 (2021)

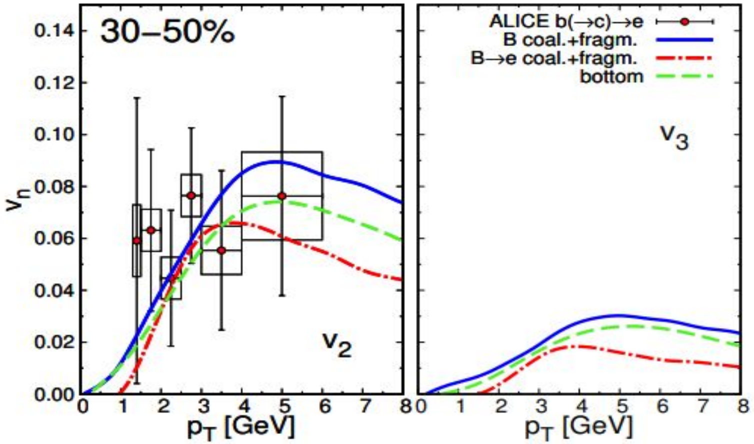

Compared to charm quark:

- Efficiency of conversion of ε_2 :
  - ➡ 15% smaller for v_2 in most central collisions.
  - ➡ 40% smaller for v_2 at 30−50% centrality.
- Efficiency of conversion of ε_3 :
  - ➡ 30% smaller for v_3 at both 0-10% and 30-50% centralities.

From central to peripheral:

- enhancement of v_2 (ε_2(0-10%)≃0.13 and ε_2(30-50%)≃0.42)
- similar v_3 (ε_3(0-10%)≃0.11 and ε_3(30-50%))≃0.21)

MOMENTUM DEPENDENT Quasi Particle Model:

QPM vs QPMp

Going back to Quasi Particle Model (QPM)...

Equation of State and Susceptibilities

Non perturbative dynamics → M scattering matrices (q,g → Q) evaluated by Quasi-Particle Model fit to **lQCD thermodynamics**

N_f=2+1
Bulk:
u,d,s

QPM Standard

no momentum dependence

$$m_g^2(T) = \frac{2N_c}{N_c^2-1} g^2(T)\,T^2$$
$$m_q^2(T) = \frac{1}{N_c} g^2(T)\,T^2$$

→ Thermal masses of gluons and light quarks

g(T) from a fit to ε from lQCD data → good reproduction of P, ε-3P

$$g^2(T) = \frac{48\pi^2}{(11N_c - 2N_f)\ln\left[\lambda\left(\frac{T}{T_c} - \frac{T_s}{T_c}\right)\right]^2}$$

λ=2.6
T_s=0.57 T_c

Larger than pQCD especially as T → T_c

Standard QPM underestimates the **quark susceptibilities**

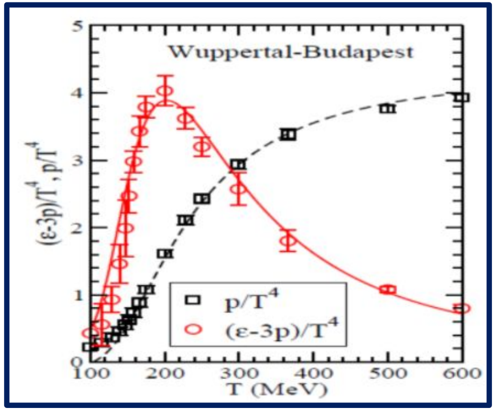

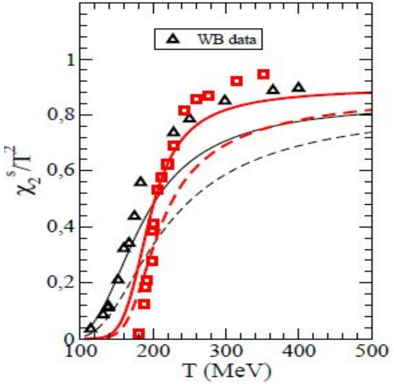

S. Plumari et al, *Phys.Rev.D* 84 (2011) 094004
H. Berrehrah,, PHYSICAL REVIEW C **93**, 044914 (2016)

QPM extension: QPMp(N_f=2+1+1)

Dyson-Schwinger studies in the vacuum → following the model developed by PHSD group

H. Berrehrah, W. et al., Phys.Rev.C 93, 044914 (2016).
C. S. Fischer, J. Phys. G 32, R253 (2006).
M.L. Sambataro et al. e-Print: 2404.17459

$$M_g(T,\mu_q,p) = \left(\frac{3}{2}\right)\left(\frac{g^2(T^\star/T_c(\mu_q))}{6}\left[\left(N_c+\frac{1}{2}N_f\right)T^2+\frac{N_c}{2}\sum_q\frac{\mu_q^2}{\pi^2}\right]\left[\frac{1}{1+\Lambda_g(T_c(\mu_q)/T^\star)p^2}\right]\right)^{1/2}+m_{\chi g}$$

$$M_{q,\bar q}(T,\mu_q,p) = \left(\frac{N_c^2-1}{8N_c}g^2(T^\star/T_c(\mu_q))\left[T^2+\frac{\mu_q^2}{\pi^2}\right]\left[\frac{1}{1+\Lambda_q(T_c(\mu_q)/T^\star)p^2}\right]\right)^{1/2}+m_{\chi q}$$

Momentum dependent factors

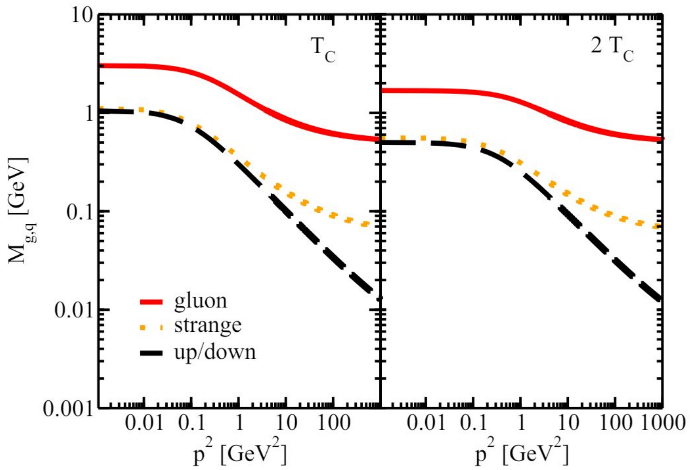

We correctly reproduce both **EoS** and **quark susceptibilities** which are understimated in the standard QPM approach.

Pressure, trace anomaly **including charm** Nf=2+1+1

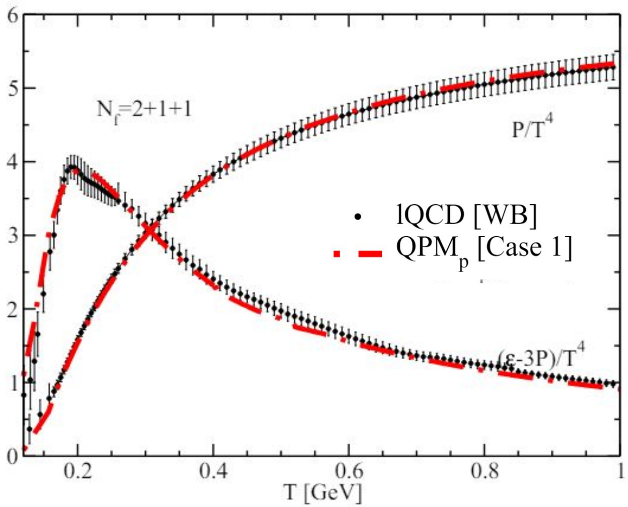

QPM extension: QPMp(N_f=2+1+1) and m_c (T)

we have also extended our quasi-particle model approach for **Nf = 2+1** to **Nf = 2 + 1 + 1** where the **charm quark is included**

Temperature parametrization for charm mass:

Case 1: $m_c = 1.5\ GeV$

Case 2: $m_c^2 = m_{c0}^2 + \frac{N_c^2-1}{8N_c} g^2 [T^2 + \frac{\mu_c^2}{\pi^2}]$ with $m_{c0} = 1.3\ GeV$

Case 3: m_c fixed by charm fluctuation $\chi_2^c = \frac{T}{V}\frac{\partial^2 \ln Z}{\partial \mu_i^2}$

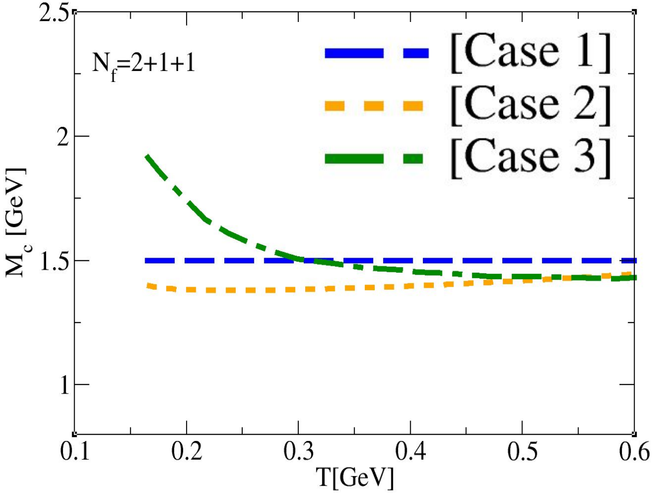

QUARK SUSCEPTIBILITIES

$$\chi_{u,s,c} = \frac{T}{V}\frac{\partial^2 \ln Z}{\partial \mu_{u,s,c}^2}$$

STRANGE

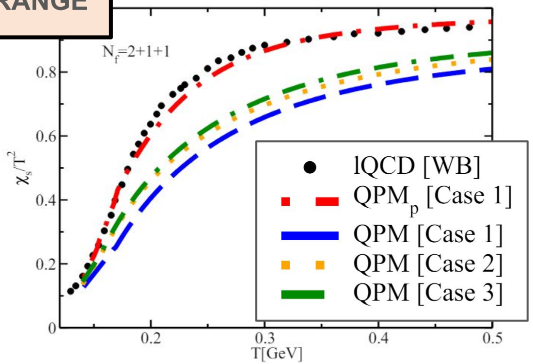

LIGHT

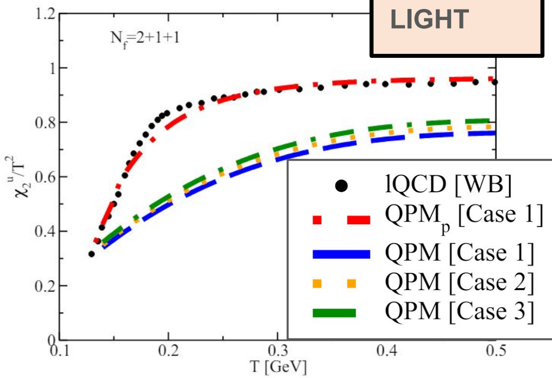

QPM understimates the lQCD data;
QPMp -> smaller 'thermal average mass' -> extra contribution in susceptibility

M.L. Sambataro et al. e-Print: 2404.17459

QPM extension: QPMp(N_f=2+1+1) and m_c (T)

we have also extended our quasi-particle model approach for **Nf = 2+1** to **Nf = 2 + 1 + 1** where the **charm quark is included**

Temperature parametrization for charm mass

Case 1: $m_c = 1.5\ GeV$

Case 2: $m_c^2 = m_{c0}^2 + \frac{N_c^2-1}{8N_c} g^2 [T^2 + \frac{\mu_c^2}{\pi^2}]$ with $m_{c0} = 1.3\ GeV$

Case 3: m_c fixed by charm fluctuation $\chi_2^c = \frac{T}{V}\frac{\partial^2 \ln Z}{\partial \mu_i^2}$

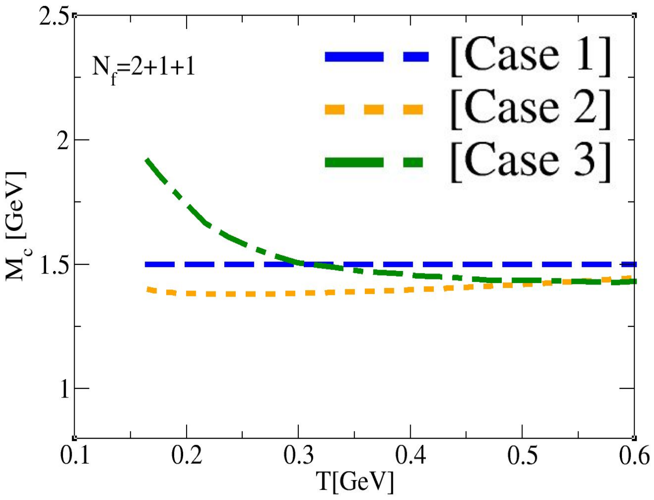

QUARK SUSCEPTIBILITIES

$$\chi_{u,s,c} = \frac{T}{V}\frac{\partial^2 \ln Z}{\partial \mu_{u,s,c}^2}$$

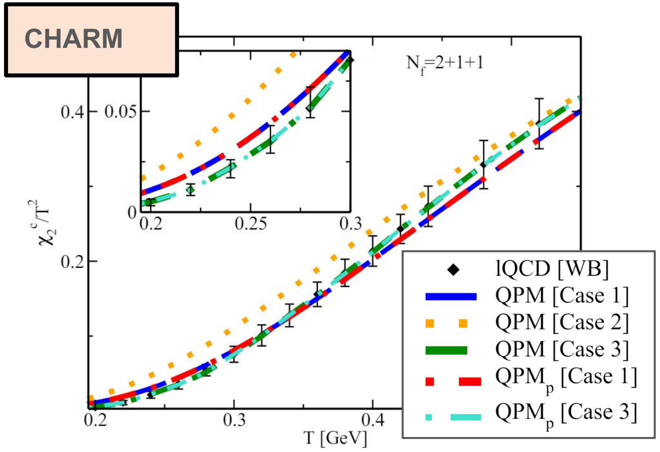

- lQCD data overestimated for T≈0.2-0.3 GeV with constant m_c.
- **Disfavored**: increasing m_c(T) and m_c smaller than 1.5 GeV
- Susceptibility implies a decreasing m_c(T) from 1.9 at T_c down to 1.5 at $2T_c$.

M.L. Sambataro et al. e-Print: 2404.17459

QPMp – spatial diffusion coefficient D_s

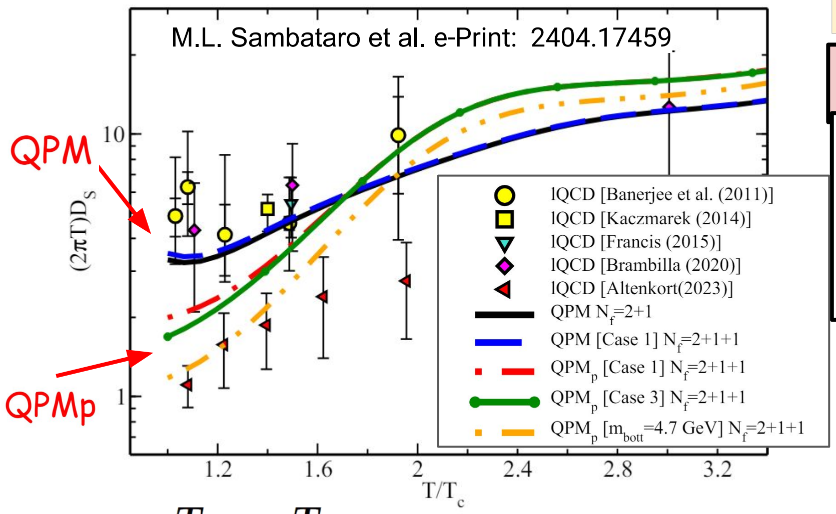

Spatial diffusion coefficient D_s → standard QPM

standard QPM including charm

extended QPM

QPMp

$T/T_c < 1.6$ -> strong non-perturbative behaviour of D_s.

high T region -> D_s grows toward the pQCD estimate faster than QPM

QPMp for charm Case 3 and bottom (M=4.7 GeV): closer to D_s lQCD which include dynamical fermions

$$D_s = \frac{T}{M\,\gamma} = \frac{T}{M}\,\tau_{th}$$

in the p → 0 limit

From D_s we obtain at T_c :

- τ_{th}(c , p=0) ~ 6 fm/c (QPM) -> 4 fm/c (QPMp)
- τ_{th}(b , p=0) ~ 13 fm/c (QPM) -> 7 fm/c (QPMp)

QPMp – spatial diffusion coefficient D_S

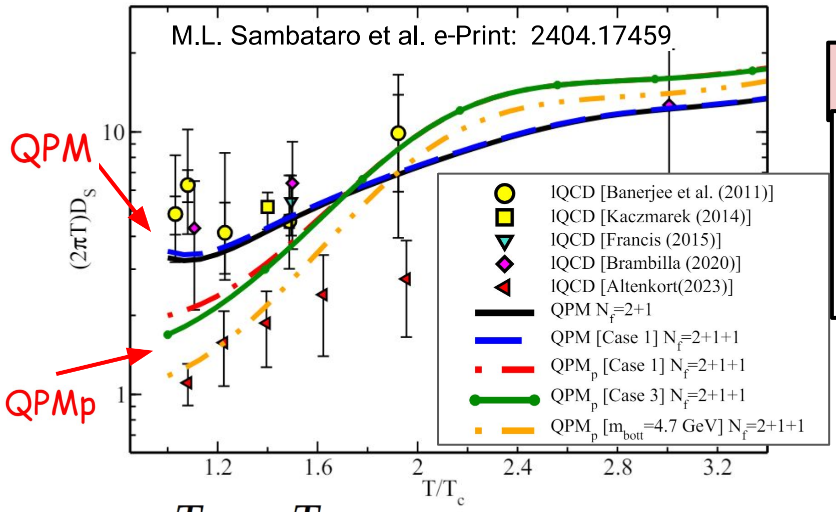

Spatial diffusion coefficient D_s → standard QPM
standard QPM including charm
extended QPM

QPMp

T/T$_c$ <1.6 -> strong non-perturbative behaviour of D_S.

high T region -> D_S grows toward the pQCD estimate faster than QPM

QPMp for charm Case 3 and bottom (M=4.7 GeV): closer to D_S lQCD which include dynamical fermions

$$D_s = \frac{T}{M\,\gamma} = \frac{T}{M}\,\tau_{th}$$

τ_{th} for charm

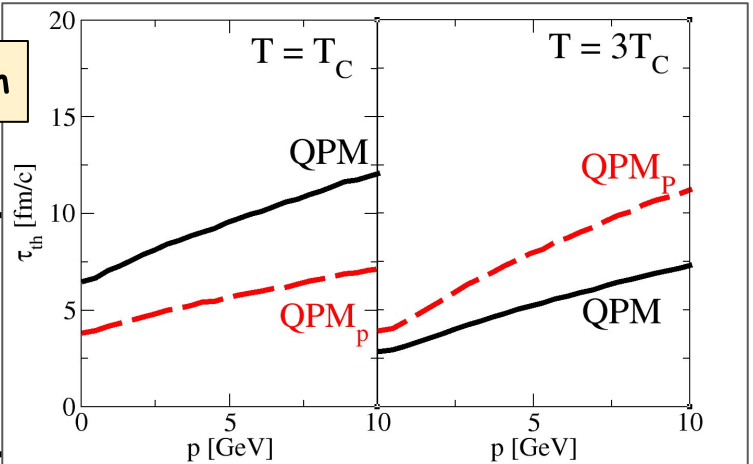

T=T$_C$ -> 40 % larger τ_{th} for both QPM and QPMp at at finite momentum (~5 GeV)

T=3T$_C$ QPMp -> more perturbative dynamics -> larger τ_{th} wrt QPM finite momentum (~5 GeV) -> 50 % larger τ_{th}

QPMp – spatial diffusion coefficient D_S

Spatial diffusion coefficient D_s → standard QPM
standard QPM including charm
extended QPM

QPMp

QPM

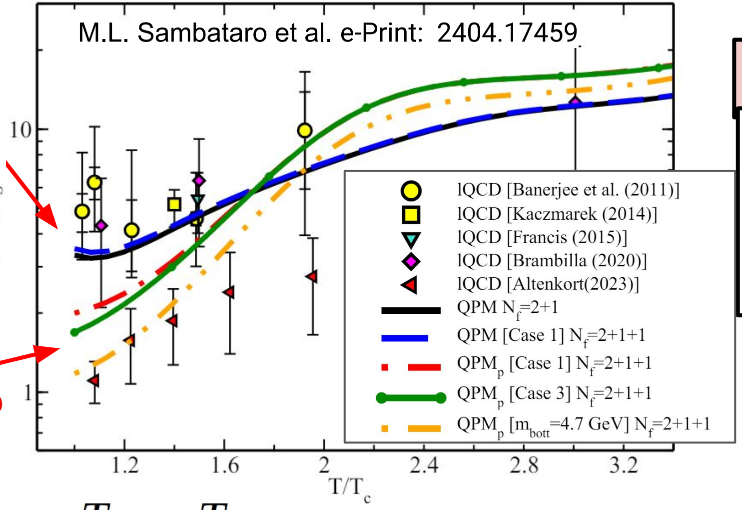

QPMp

T/T_c <1.6 -> strong non-perturbative behaviour of D_S.
high T region -> D_S grows toward the pQCD estimate faster than QPM

QPMp for charm Case 3 and bottom (M=4.7 GeV): closer to D_S lQCD which include dynamical fermions

$$D_s = \frac{T}{M\,\gamma} = \frac{T}{M}\,\tau_{th}$$

QPM/QPMp use finite mass and includes dynamical fermions

QPM vs QPMp in the infinite mass limit?

standard QPM

extended QPM

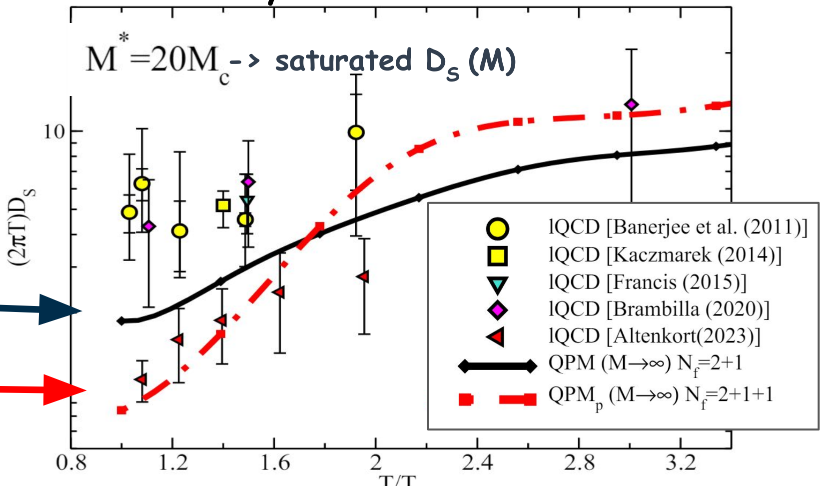

bottom (M=4.7 GeV): very close to infinite mass limit

QPMp – spatial diffusion coefficient D_S

Spatial diffusion coefficient D_s → standard QPM

standard QPM including charm

extended QPM

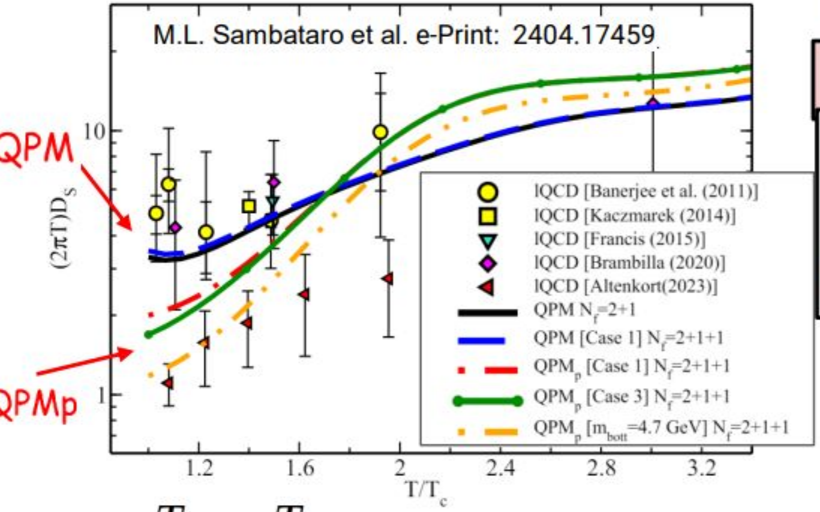

QPMp

T/T_c <1.6 -> strong non-perturbative behaviour of D_S.

high T region -> D_S grows toward the pQCD estimate faster than QPM

$$D_s = \frac{T}{M\gamma} = \frac{T}{M}\tau_{th}$$

$$T = T_0(t/t_0)^{-\frac{1}{3}}$$

Initial momentum distribuction function

→ FONLL for charm quark

$$R_{AA} \doteq f_C(p,t_f)/f_C(p,t_0)$$

QPM vs QPMp

-> R_{AA} reduction especially for **Case 3**

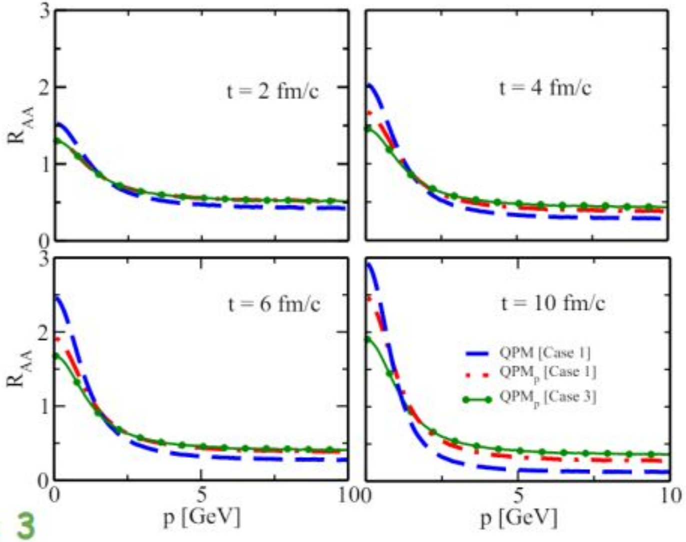

Conclusions

- **Extension to bottom quark dynamics in standard QPM**: good description of R_{AA} and v_2 of electrons from semileptonic B meson decay and prediction for v_2 and v_3

- **Charm mass [T] parametrization:** charm susceptibility as function of T implies a decreasing m_C(T) from 1.9 at T_C down to 1.5 at $2T_C$ getting closer to lQCD data for Ds.

- **QPMp**
  Good reproduction of both EoS and susceptibilities -> decrease of D_s at small T.
  Bottom D_s very close to the new lQCD data for M->∞.
- **Spatial diffusion coefficient D_s(T) in the infinite mass limit ->** satisfactory agreement with the lQCD calculations that include dynamical fermions, differently from previous lQCD data in quenched approximation.

  - Perspectives: Effect on observables for realistic simulations.

Thanks for the attention!

Back up slides

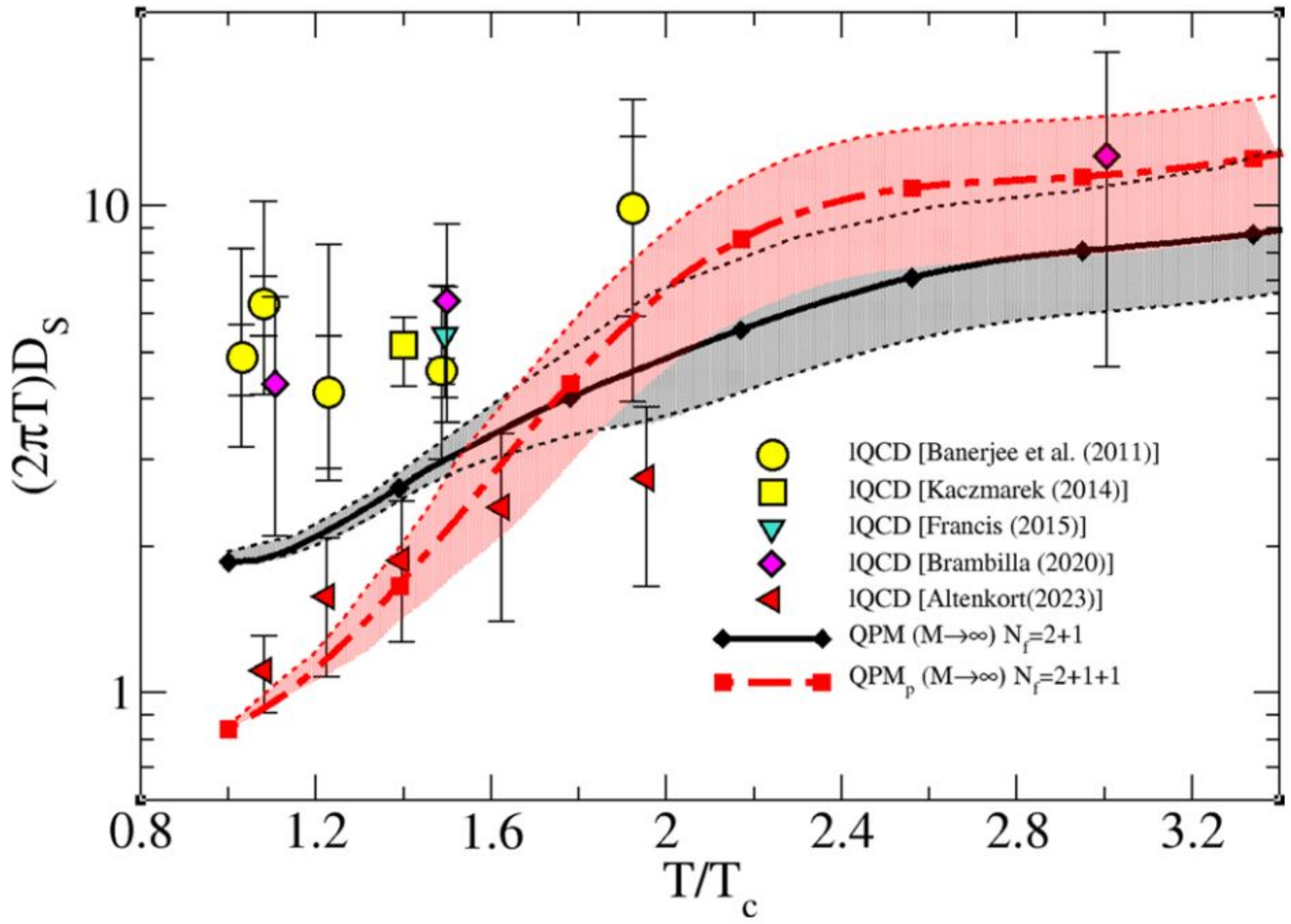

10
1
0.8
1.2
1.6
2
2.4
2.8
3.2
T/T_c
(2πT)D_S
lQCD [Banerjee et al. (2011)]
lQCD [Kaczmarek (2014)]
lQCD [Francis (2015)]
lQCD [Brambilla (2020)]
lQCD [Altenkort(2023)]
QPM (M→∞) N_f=2+1
QPM_p (M→∞) N_f=2+1+1

Non-perturbative effects: impact of off-shell dynamics QPM vs. DQPM

- Partons are dressed by non-perturbative spectral functions:

$$A_i^{BW}(m_i) = \frac{2}{\pi} \frac{m_i^2 \gamma_i^*}{(m_i^2 - M_i^2)^2 + (m_i \gamma_i^*)^2}$$

$$C[f] = \int dm_i A(m_i) \int dm_f A(m_f) \times \frac{1}{2E_p} \int \frac{d^3\mathbf{q}}{2E_q(2\pi)^3} \int \frac{d^3\mathbf{q}'}{2E_{q'}(2\pi)^3} \int \frac{d^3\mathbf{p}'}{2E_{p'}(2\pi)^3} \times \frac{1}{\gamma_Q} \sum |\mathcal{M}_Q|^2 (2\pi)^4 \delta^4(p+q-p'-q') \times [f(\mathbf{p}')\hat{f}(\mathbf{q}', m_f) - f(\mathbf{p})\hat{f}(\mathbf{q}, m_i)]$$

Evaluated in DQPM approach

For references: W. Cassing, Nucl.Phys. A831, 215
E. Bratkovskaya, Nucl.Phys. A856, 162
H. Berrehrah, Phys. Rev. C 89(5), 054901
M.L. Sambataro et al., *Eur.Phys.J.C* 80 12, 1140

Off-shell≈ PHSD but also larger widths!

Bulk is not with the same energy density
The energy density of off-shell case is smaller

- Transport coefficient scales with energy density of the system ε
- Larger breaking for low p region ($p \lesssim$2-3 GeV/c)
  → **larger off-shell effects**
  →30-40% decreasing drag

BOX CALCULATION [T=200 MeV] FOR CHARM

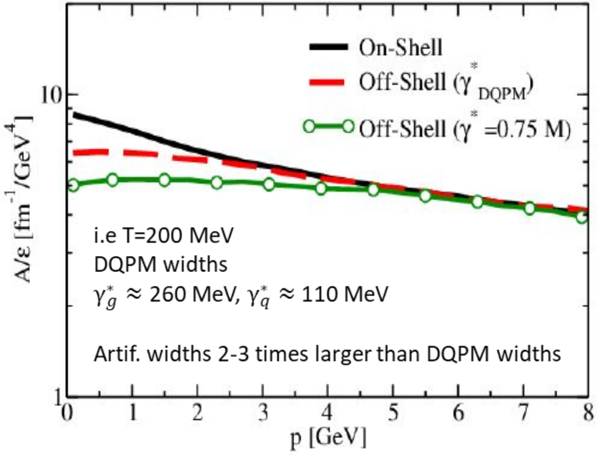

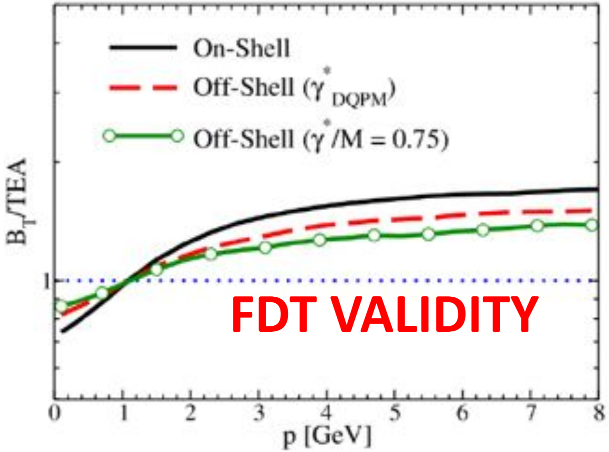

On-shell vs Off-shell energy loss

BOX CALCULATION [T=200 MeV] FOR CHARM

- Partons are dressed by non-perturbative spectral functions:

$$A_i^{BW}(m_i) = \frac{2}{\pi} \frac{m_i^2 \gamma_i^*}{(m_i^2 - M_i^2)^2 + (m_i \gamma_i^*)^2}$$

Boltzmann equation and off-shell extension

$p^\mu \partial_\mu f_Q = C[f_Q, f_{g,q}]$

Plasma uniform $\rightarrow$ $p^0 \partial_0 f_Q = C[f_Q, f_{g,q}]$

$\frac{\partial f_Q}{\partial t} = \frac{1}{E_Q} C[f_q, f_g, f_Q]$

$f(t + \Delta t, p) = f(t, p) + \frac{1}{E_Q} C[f]$

$C[f_q, f_g, f_Q]$ Collision integral calc. both in on-shell and off-shell mode

$\varepsilon_{onshell} = \varepsilon_{offshell}$

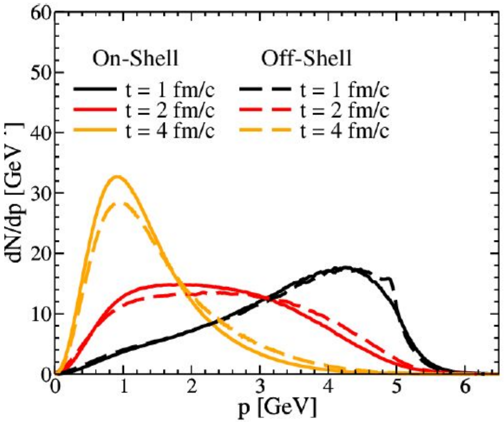

+k(p) making the Drag on-shell=Drag off-shell

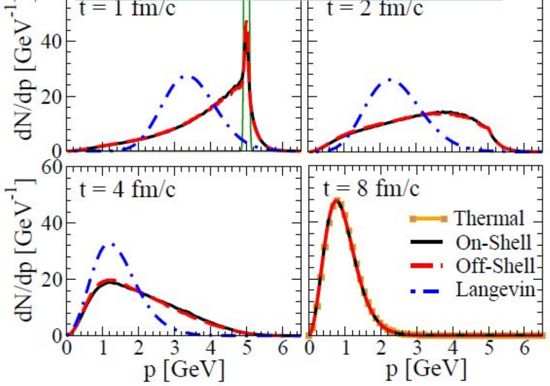

The difference between on-shell and off-shell mode can be adsorbed by multiplying scattering matrix for a *k* factor

QPMp – D_S and R_{AA}

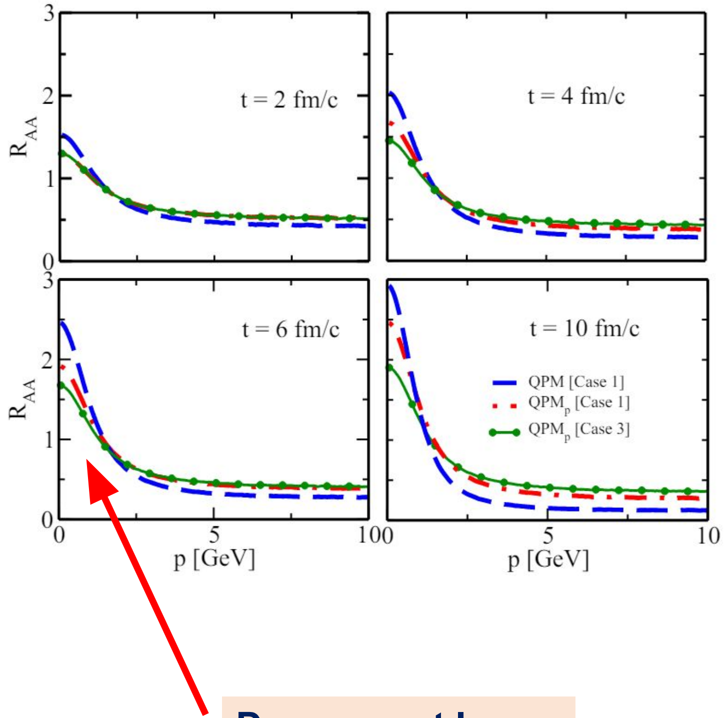

Decrease at low p

1+1D system $T = T_0(t/t_0)^{-\frac{1}{3}}$

Initial momentum distribution function
→ FONLL for charm quark

$$R_{AA} \doteq f_C(p,t_f)/f_C(p,t_0)$$

QPM vs QPMp -> R_{AA} reduction especially for **Case 3**

Momentum dependent QPM approach

- Better description of recent lQCD data.
- Effects on the global χ^2 coming from the comparison to the experimental data of R_{AA}, v_n?

M.L. Sambataro et al. e-Print: 2404.17459

QPM extended – QPMp + m_c (T)

we have also extended our quasi-particle model approach for **Nf = 2+1** to **Nf = 2 + 1 + 1** where the **charm quark is included**

Temperature parametrization for charm mass

Case 1: $m_c = 1.5\ GeV$

Case 2: $m_c^2 = m_{c0}^2 + \frac{N_c^2-1}{8N_c} g^2 [T^2 + \frac{\mu_c^2}{\pi^2}]$ with $m_{c0} = 1.3\ GeV$

Case 3: m_c fixed by charm fluctuation $\chi_2^c = \frac{T}{V}\frac{\partial^2 \ln Z}{\partial \mu_i^2}$

The following expression for the quark fluctuations:

$$c_2^q = \frac{\chi_2^q}{2} = \frac{1}{2}\frac{6}{\pi^2}\left(\frac{m_q}{T}\right)^2 \sum_{l=1}^{\infty} (-1)^{l+1} K_2(l m_q/T)$$

can be solved in terms of mq/T , with the χ values numerically obtained in lQCD. We then fit the resulting temperature dependence of charm mass

M.L. Sambataro et al. e-Print: 2404.17459

QPM extended – QPMp

Dyson-Schwinger studies in the vacuum → following the model developed by PHSD group

H. Berrehrah, W. et al., Phys.Rev.C 93, 044914 (2016).
C. S. Fischer, J. Phys. G 32, R253 (2006).
M.L. Sambataro et al. e-Print: 2404.17459

$$M_g(T,\mu_q,p) = \left(\frac{3}{2}\right)\left(\frac{g^2(T^\star/T_c(\mu_q))}{6}\left[\left(N_c + \frac{1}{2}N_f\right)T^2 + \frac{N_c}{2}\sum_q \frac{\mu_q^2}{\pi^2}\right]\left[\frac{1}{1+\Lambda_g(T_c(\mu_q)/T^\star)p^2}\right]\right)^{1/2} + m_{\chi g}$$

$$M_{q,\bar{q}}(T,\mu_q,p) = \left(\frac{N_c^2-1}{8N_c}g^2(T^\star/T_c(\mu_q))\left[T^2 + \frac{\mu_q^2}{\pi^2}\right]\left[\frac{1}{1+\Lambda_q(T_c(\mu_q)/T^\star)p^2}\right]\right)^{1/2} + m_{\chi q}$$

Momentum dependent factors

We correctly reproduce both **EoS** and **quark susceptibilities** which are understimated in the standard QPM approach.

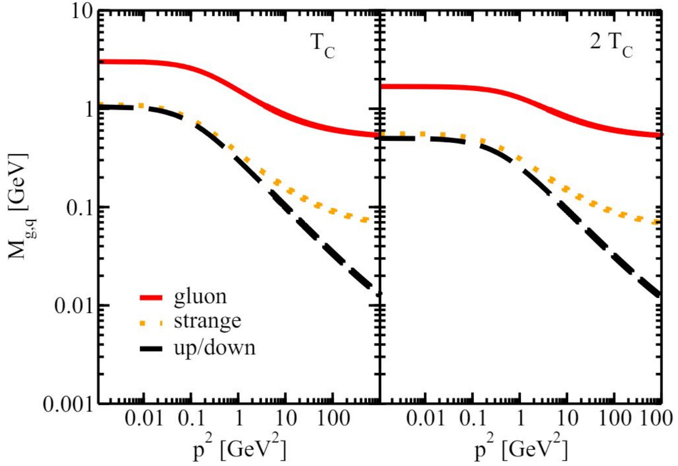

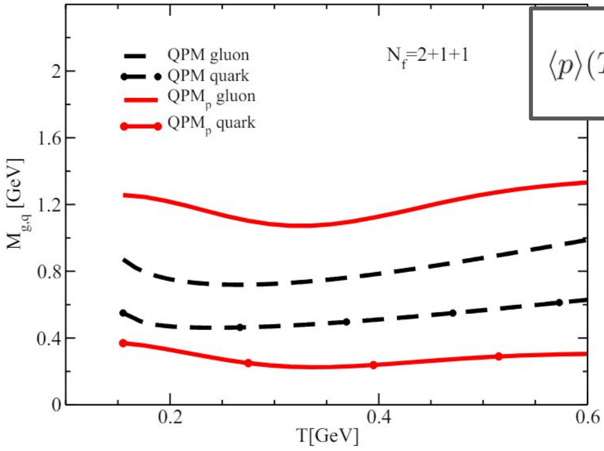

$$\langle p\rangle(T) = \frac{\int_0^\infty |\vec{p}| f_i(\vec{p},T)d^3p}{\int_0^\infty f_i(\vec{p},T)d^3p}$$

m_g/m_q in QPMp is larger by a factor 2 wrt QPM

ESE: $v_n - v_m$ correlations

M.L. Sambataro, et al., *Eur.Phys.J.C* 82 (2022)

Charged particles

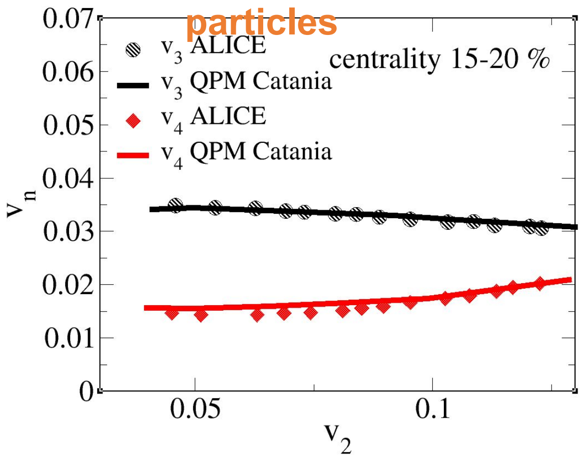

Predictions for D

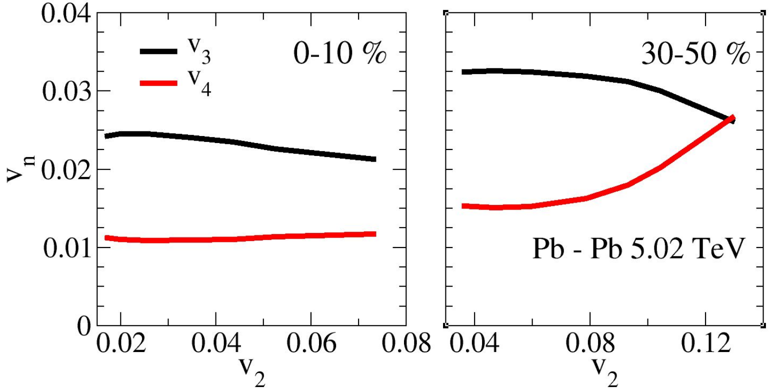

Correlations between the ε_n and ε_m present in the initial geometry → correlations between flow harmonics different orders, i.e. correlations v_n and v_m

- Good description of $v_{n\text{-}m}$ correlation for bulk
- Prediction for similar correlation for hard particles
- Correlation for D mesons provide insights on the interaction and its temperature dependence

Plumari et al, Phys.Lett.B 805 (2020) 135460

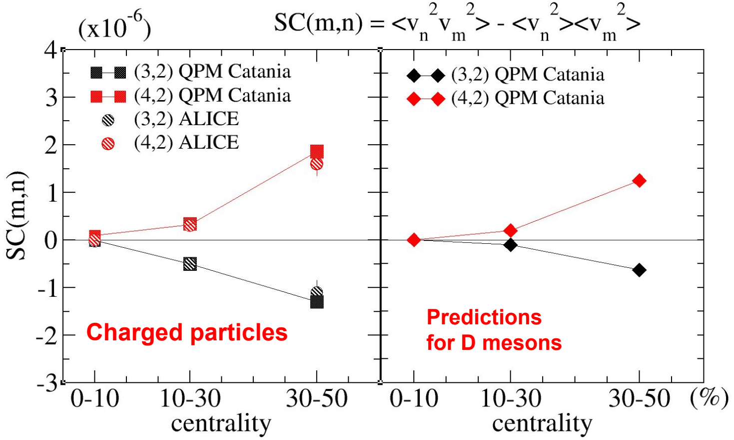

Data taken from: S. Mohapatra *Nucl.Phys.A* 956 (2016) 59-66

QPM extended – Preliminary D_S and R_{AA}

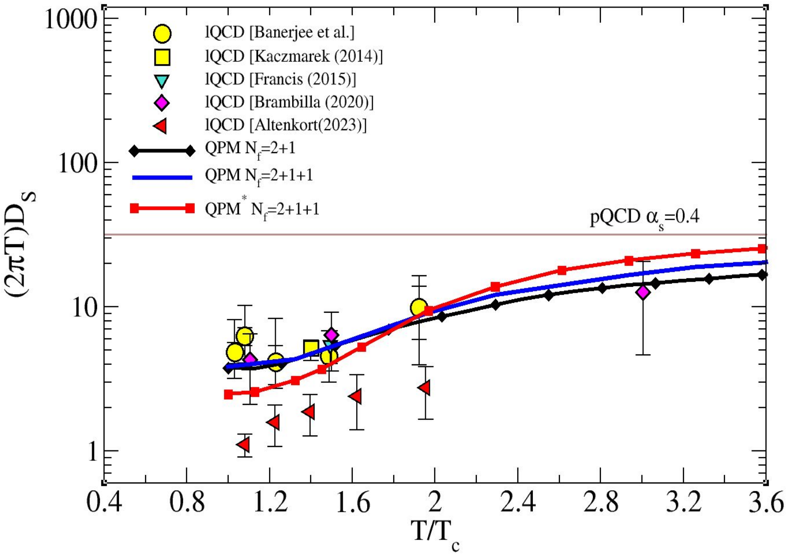

Spatial diffusion coefficient D_s → standard QPM

standard QPM including charm

extended QPM

$T/T_c < 2$ → strong non-perturbative behaviour near to T_c.

high T region → the D_s reaches the pQCD limit quickly than the standard QPM.

coupling g(T)

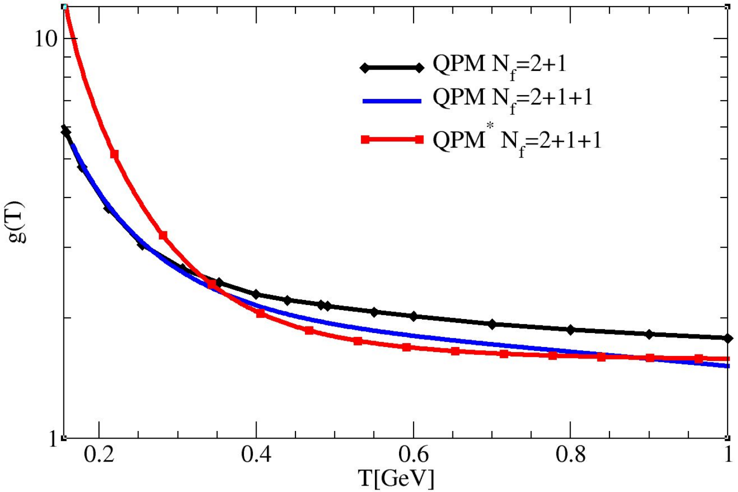

D meson: Impact of large Λ_c production on R_{AA}

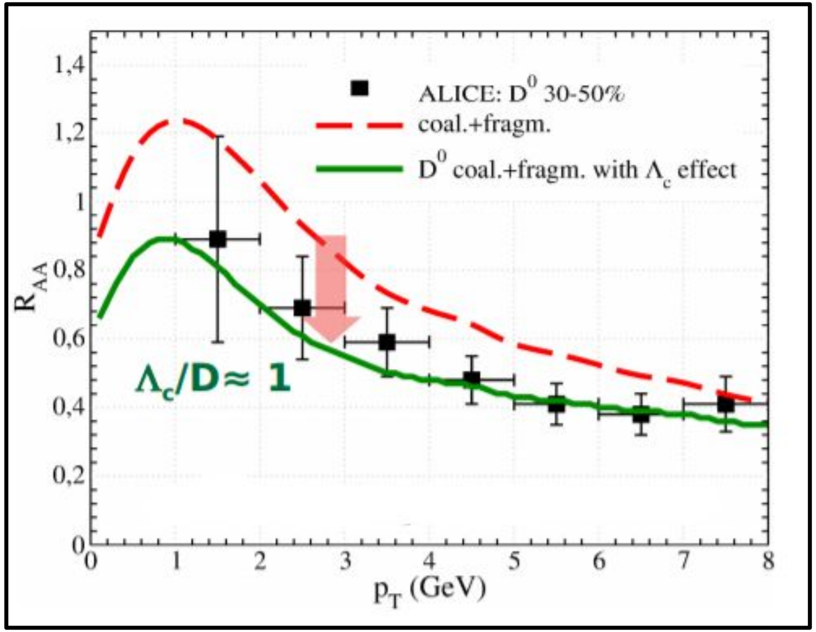

$D_s(T)$ of charm quark that reproduces R_{AA} and v_2 gives good description of

- Impact of Λ_C / D^0
- Triangular flow $v_3(p_T)$.
- q_2 selected anisotropic flow and spectra.

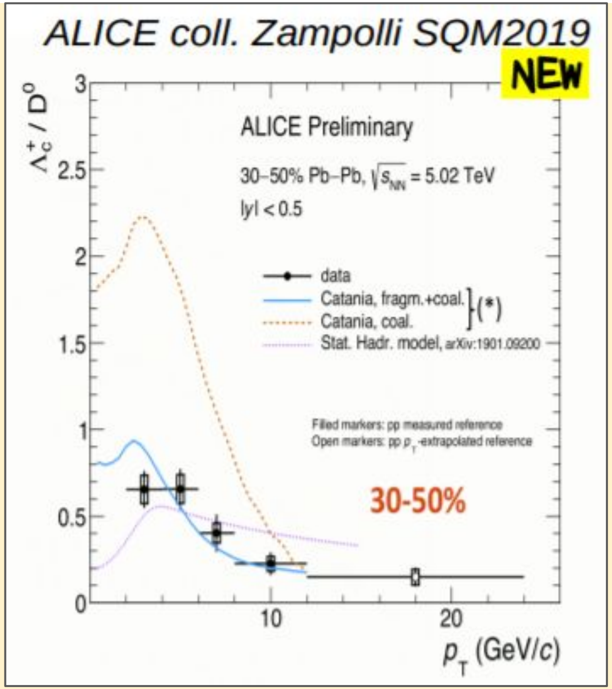

- With the same coalescence plus fragmentation model we describe the Λ_C / D^0

S. Plumari, et al.,
Eur. Phys. J. C78 no. 4, (2018) 348

$(2\pi T)D_s$: Charm quark vs Bottom quark

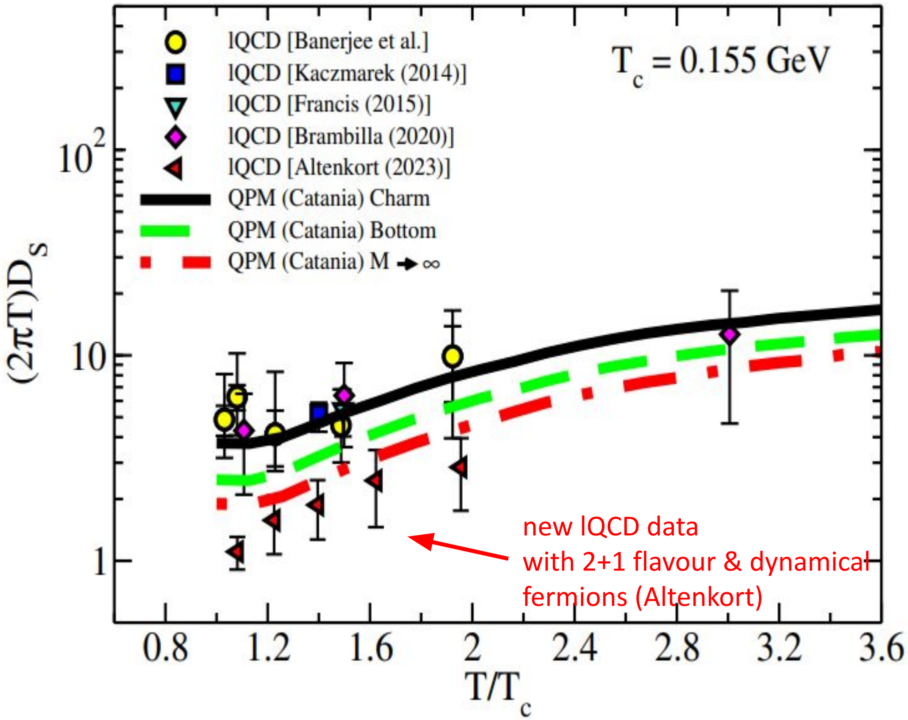

- lQCD data are in $M_Q \rightarrow \infty$, so the D_s evaluated is mass independent + quenched medium
- QPM use finite mass and includes dynamical fermions

$$D_s = \frac{T}{M\,\gamma} = \frac{T}{M}\,\tau_{th}$$

From kinetic theory is expected that:

$$\tau_{th}(b)/\,\tau_{th}(c) \approx \gamma_c/\,\gamma_b \approx M_b/M_c$$

In QPM approach $\rightarrow D_s(c)$ is 30-40% larger than $D_s(b)$ (no mass independence)

$M \rightarrow \infty$ limit is not reached for charm

From D_s we obtain (in the 1-2T_c range):

- $\tau_{th}(c)$ ~ 5 fm/c
- $\tau_{th}(b)$ ~ 11 fm/c   breaking w.r.t. the relation:

  $\tau_{th}(b) = (M_b/M_c)\tau_{th}(c)$ ~ 3.3 $\tau_{th}(c)$ ~ 16.5 fm/c

M.L. Sambataro et al., e-Print: 2304.02953

$(2\pi T)D_s$ ratios: Charm quark vs Bottom quark

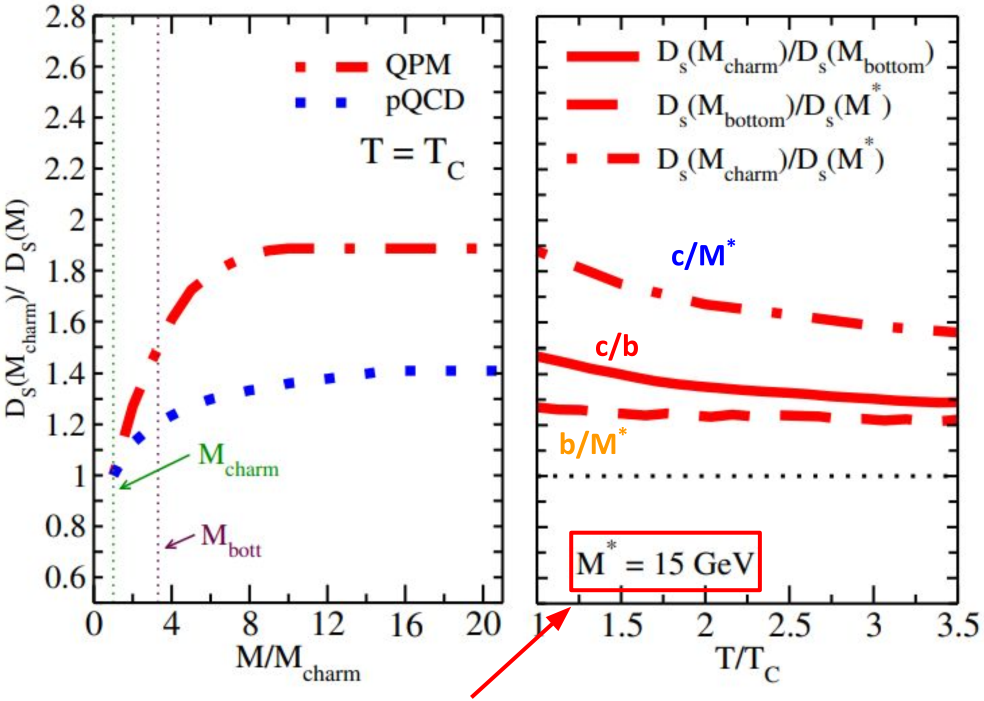

fictitious super-heavy quark staying in the $M_Q \to \infty$ limit

➢ $D_s(M_{charm})/D_s(M)$ as a function of M/M_{charm} at T_C:

Saturation scale of Ds for $M_Q \sim 8\, M_{charm} \gtrsim 10$ GeV
$Ds(M_{charm})/Ds(M \to \infty) = 1.9$ for QPM.

$Ds(M_{charm})/Ds(M \to \infty) \simeq 1.4$ for pQCD.

➢ Ratios at fixed mass as a function of T:

- **b/M^*: about 25% in all T range**
- **c/b: about 50% at T_C and not smaller than 30%**
- **c/M^*: factor 1.5-2**

M.L. Sambataro et al., e-Print: 2304.02953

$(2\pi T)D_s$: Charm quark vs Bottom quark

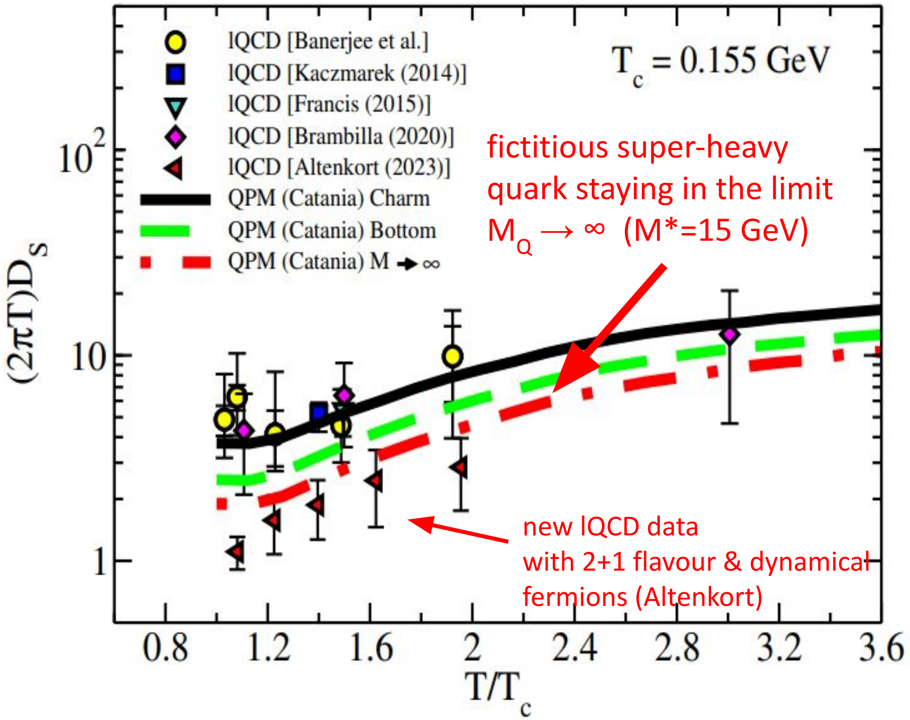

- lQCD data are in $M_Q \to \infty$ so D_s is mass independent

$$D_s = \frac{T}{M\,\gamma} = \frac{T}{M}\,\tau_{th}$$

- QPM use finite mass and includes dynamical fermions

From kinetic theory is expected that:

$$\tau_{th}(b)/\tau_{th}(c) \approx \gamma_c/\gamma_b \approx M_b/M_c$$

From D_s we obtain (in the 1-2T_c range):

- $\tau_{th}(c)$ ~ 5 fm/c
- $\tau_{th}(b)$ ~ 11 fm/c   breaking w.r.t. the relation:
  $\tau_{th}(b) = (M_b/M_c)\tau_{th}(c)$ ~ 3.3 $\tau_{th}(c)$ ~ 16.5 fm/c

$D_s(T)$ from QPM in the infinite mass limit is the more pertinent to compare to lQCD simulations evaluated taking into account dynamical fermions

M.L. Sambataro et al., e-Print: 2304.02953

Ds mass dependence: QPM vs QPMp

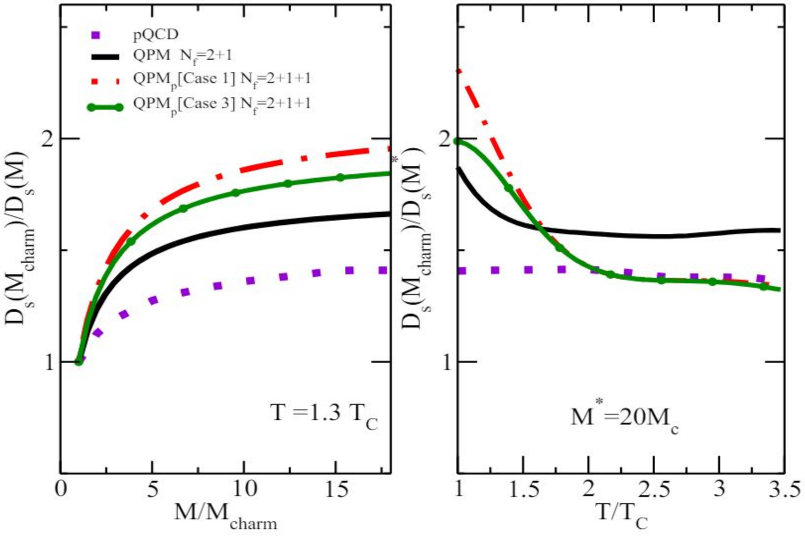

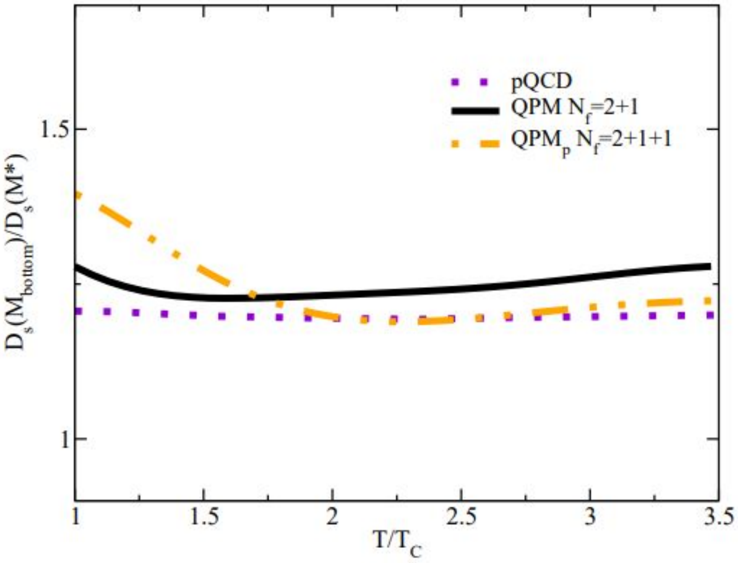

Numerical solution of Boltzmann Equation

- **Use Test-Particle Method to sample the phase space distribution function**

$$f(\vec{x},\vec{p},t)=\omega\sum_{i=1}^{N_{test}}\delta^{(3)}(\vec{x}-\vec{r}_i(t))\delta^{(3)}(\vec{p}-\vec{p}_i(t))$$

F_i solution of Boltzmann eq.
→ Test particles solve classical Hamilton eq. of motion

$$\begin{cases}\vec{p}_i(t+\Delta t)=\vec{p}_i(t-\Delta t)+2\Delta t\cdot\left(\frac{\partial\vec{p}_i}{\partial t}\right)_{coll}\\ \vec{r}_i(t+\Delta t)=\vec{r}_i(t-\Delta t)-2\Delta t\cdot\left[\frac{\vec{p}_i(t)}{E_i(t)}\right]\end{cases}$$

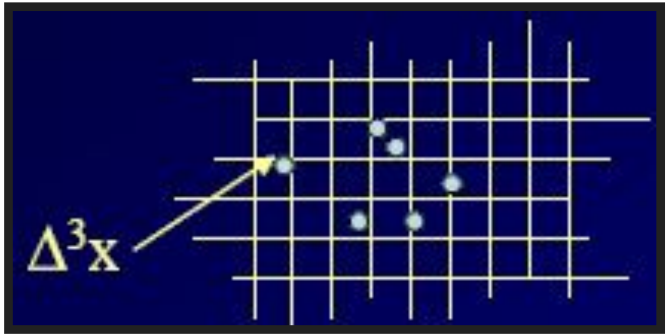

- **Collision Integral mapped through a Stochastic Al**

Δt □ 0 and Δ^3x □ 0 : exact solution

$$P_{22}=\frac{\Delta N_{coll}^{2\to2}}{\Delta N_1\Delta N_2}=v_{rel}\sigma_{22}\frac{\Delta t}{\Delta^3 x}$$

Final phase-space of HQ + bulk parton scattering sampled according to $|M_{QCD}|^2$ □ code test through simulations in a “box”

[Scardina, Colonna, Plumari, and Greco PLB v.724, 296 (2013)]
[Xu and Greiner PRC v. 71, (2005)]

Hybrid Hadronization Model for HQs

✔ **COALESCENCE**: Formula developed for the light sector **[Greco, Ko, Levai PRL 90 (2003)]**

$$\frac{dN_H}{d^2\boldsymbol{P}_T} = g_H \int \prod_{i=1}^{n} \frac{d^3 p_i}{(2\pi)^3 E_i} p_i \cdot d\sigma_i \, f_{q_i}(x_i, p_i) \, f_W(x_1 \ldots x_n; p_1 \ldots p_n) \, \delta\left(\boldsymbol{P_T} - \sum_i^n p_{T,i}\right)$$

Statistical Factor
Color-spin-isospin

Parton Distribution Functions
(after Boltzmann evolution)

Hadron Wigner Function
(parameters fix according to quark model)
C.-W. Hwang, EPJ C23, 585 (2002)
C. Albertus et al., NPA 740, 333 (2004)

✔ **FRAGMENTATION**: HQs that do not undergo to Coalescence

$$\frac{dN_H}{d^2\boldsymbol{P}_T} = \sum_f \int dz \frac{dN_f}{d^2 p_T} \frac{D_{f\to H}(z)}{z^2}$$

We use Peterson parametrization: $D_H(z) \propto \left[z\left(1 - \frac{1}{z} - \frac{\epsilon_c}{1-z}\right)^2\right]^{-1}$ *Peterson et al. PRD 27 (1983) 105*

Parameter ε_c tuned to reproduce *D* and *B* meson spectra in pp collisions.

Plumari, Minissale, Das , Coci , Greco, EPJ C 78 (2018) no.4

Relativistic Boltzmann equation at finite η/s

Bulk evolution

$$p^\mu \partial_\mu f_q(x,p) + m(x)\partial^x_\mu m(x)\partial^\mu_p f_q(x,p) = C[f_q, f_g]$$
$$p^\mu \partial_\mu f_g(x,p) + m(x)\partial^x_\mu m(x)\partial^\mu_p f_g(x,p) = C[f_q, f_g]$$

Free-streaming

field interaction
$\varepsilon - 3p \neq 0$

Collision Integral gauged to reproduce viscous Hydro at fixed η/s by means of Chapman-Ensksog

$$\sigma(n(\vec{x}),T) = \frac{1}{15}\frac{\langle p\rangle_0}{g(a)n(\vec{x})}\frac{1}{\eta/s}$$

Equivalent to viscous hydro at $\eta/s \approx 0.1$

HQ evolution

$$p^\mu \partial_\mu f_Q(x,p) = C[f_q, f_g, f_Q]$$

$$C[f_q,f_g,f_Q] = \frac{1}{2E_1}\int\frac{d^3p_2}{2E_2(2\pi)^3}\int\frac{d^3p_1'}{2E_1'(2\pi)^3}$$
$$\times[f_Q(p_1')f_{q,g}(p_2') - f_Q(p_1)f_{q,g}(p_2)]$$
$$\times|M_{(q,g)\to Q}(p_1p_2 \to p_1'p_2')|$$
$$\times(2\pi)^4\delta^4(p_1+p_2-p_1'-p_2')$$

Feynmann diagrams at first order pQCD for HQs-bulk interaction:

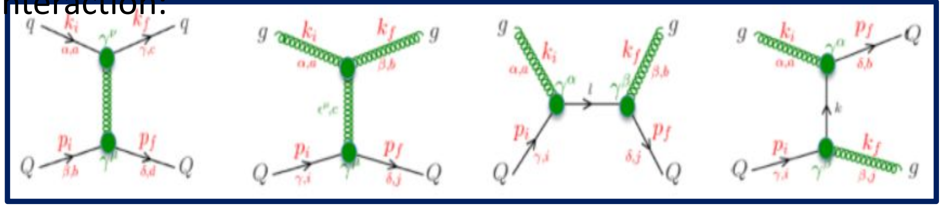

Scattering matrices $M_{g,q}$ by QPM fit to lQCD thermodynamics

Spatial diffusion coefficient of charm quark

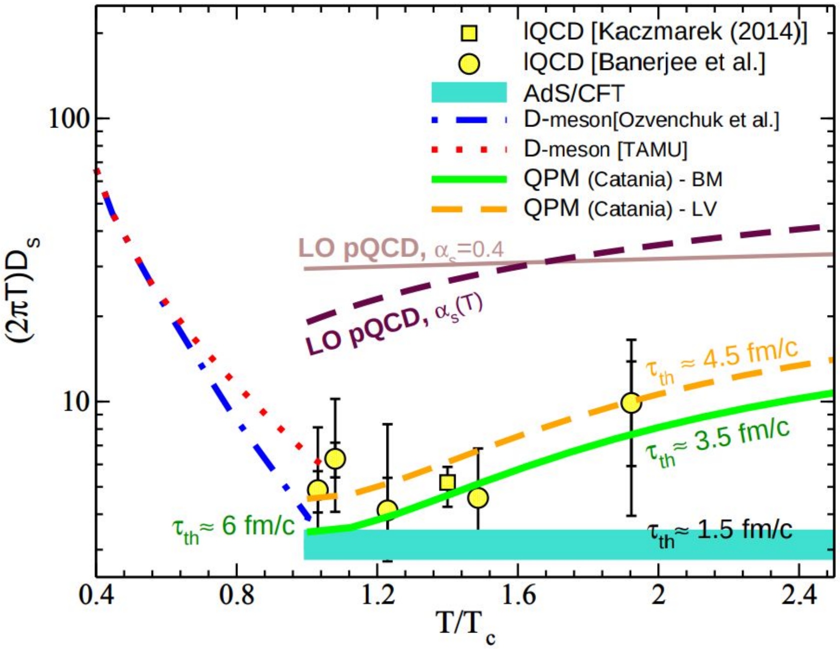

Not a model fit to lQCD data, but D_s estimate that comes from results of R_{AA} (p_T) and v_2 (p_T)

We have a probe with $\tau_{therm} \approx \tau_{QGP}$

$$\tau_{th} = \frac{M}{2\pi T^2}(2\pi T D_s) \cong 1.8 \frac{2\pi T D_s}{(T/T_c)^2} \text{ fm/c}$$

FUTURE:
-Access low p and precision data (detector upgrade)
-Better insight into hadronization
-New observables
-Bottom → **Main focus of this talk**

Reviews :
- F. Prino and R. Rapp, JPG(2019)
- X. Dong and V. Greco, Prog.Part.Nucl.Phys. (2019)
- Jiaxing Zhao et al., arXiv:2005.08277